

# Diphenyl Derivatives of Dinaphtho[2,3-*b*:2',3'-*f*]thieno[3,2-*b*]thiophene: Organic Semiconductors for Thermally Stable Thin-Film Transistors

Myeong Jin Kang,<sup>†</sup> Eigo Miyazaki,<sup>†</sup> Itaru Osaka,<sup>†</sup> Kazuo Takimiya,<sup>\*,†,‡</sup> and Akiko Nakao<sup>§</sup>

<sup>†</sup>Department of Applied Chemistry, Graduate School of Engineering, Hiroshima University, Higashi-hiroshima, Hiroshima 739-8527 Japan

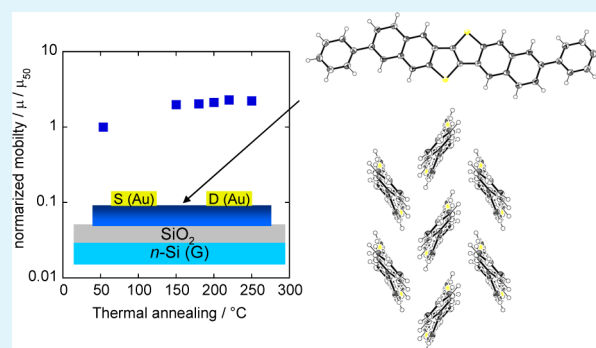
<sup>‡</sup>Emergent Molecular Function Research Team, RIKEN Advanced Science Institute, Wako, Saitama 351-0198, Japan

<sup>§</sup>High Energy Accelerator Research Organization (KEK), 1-1 Oho, Tsukuba, Ibaraki 305-0801, Japan

## Supporting Information

**ABSTRACT:** Two isomeric diphenyl-dinaphtho[2,3-*b*:2',3'-*f*]thieno[3,2-*b*]thiophene (DPh-DNTTs), 2,9- and 3,10-DPh-DNTT, were characterized by means of single-crystal X-ray analysis, thin film XRDs, and evaluation of organic field-effect transistors (OFETs) using their evaporated thin films. The packing structures both in the single crystal and thin film state were classified into a typical herringbone packing regardless of the substitution positions, similar to the parent DNTT. The OFETs showed typical p-channel transistor characteristics with mobilities of as high as  $3.5 \text{ cm}^2 \text{ V}^{-1} \text{ s}^{-1}$  for both isomers, which is slightly higher than that of the parent DNTT. Compared to related DNTT-based organic semiconductors, a unique point of DPh-DNTTs was found to be superior thermal stability in OFET devices. In particular, the 2,9-DPh-DNTT-based OFETs preserved its superior FET characteristics up to 250 °C. For its excellent thermal stability with good FET characteristics, 2,9-DPh-DNTT can be a useful organic semiconductor in various applications that require processes at high temperatures.

**KEYWORDS:** organic field-effect transistors, thienoacene-based organic semiconductors, high mobility, thermal stability, crystal structures, structure–property relationship



## INTRODUCTION

Recent progresses in organic field-effect transistor have largely relied on materials developments along with the improvement of device processing techniques.<sup>1</sup> For example poor air-stability of conventional pentacene-based OFETs has been overcome by materials with low-lying HOMO energy levels.<sup>2</sup> In addition, higher mobilities than those of pentacene-based OFETs are achieved by new materials possessing better self-assembling characteristics in the thin film state.<sup>3</sup> Dinaphtho[2,3-*b*:2',3'-*f*]thieno[3,2-*b*]thiophene (DNTT, Figure 1)<sup>4</sup> and its derivatives<sup>5</sup> are one of such organic semiconductors recently developed. Because of their good stability and performances, several attractive device applications, including OFET arrays driving a liquid crystalline display, electronic watermarks on banknotes, and flexible transistor arrays for medical applications, have been demonstrated.<sup>6</sup> In these advanced application of the DNTT-based OFETs, thermal stability of the active semiconducting layer in OFETs is emerging as an additional requirement for further sophisticated device applications.<sup>6c</sup> In this context, DNTT has been shown to be a potential material for a thermally stable transistor: Someya, Sektiani, and their co-workers have recently demonstrated sterilizable, i.e., amenable

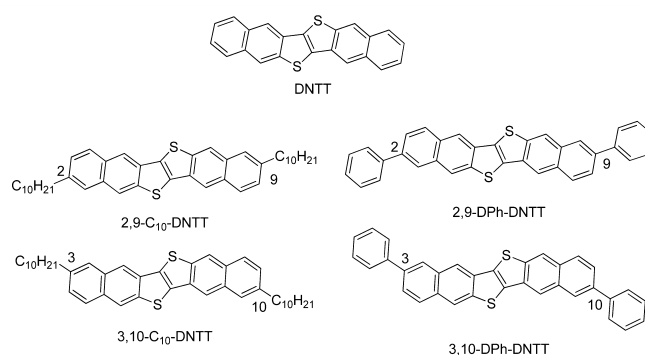


Figure 1. Molecular structures of DNTT derivatives.

**Special Issue:** Forum on Advancing Technology with Organic and Polymer Transistors

**Received:** November 7, 2012

**Accepted:** January 21, 2013

**Published:** February 14, 2013

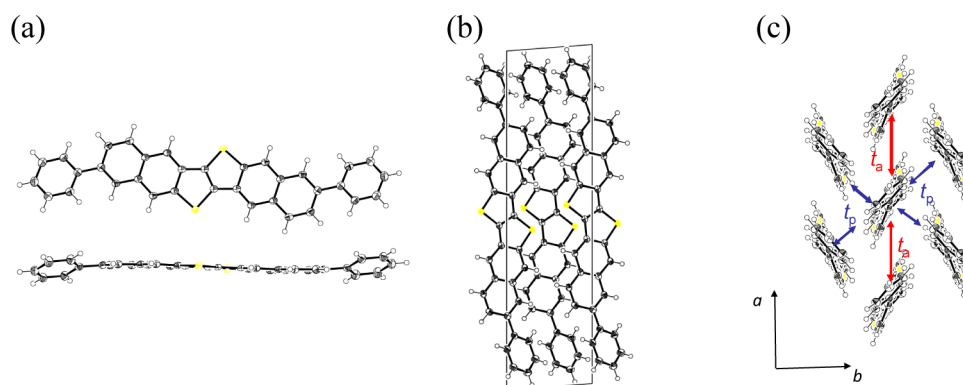


**Figure 2.** (a) Molecular structure, (b) *a*-axis projection of packing structure, and (c) packing structure in the crystallographic *ab*-plane with calculated transfer integrals:  $t_a = 52$  meV and  $t_p = 45$  meV, respectively of 2,9-DPh-DNTT.

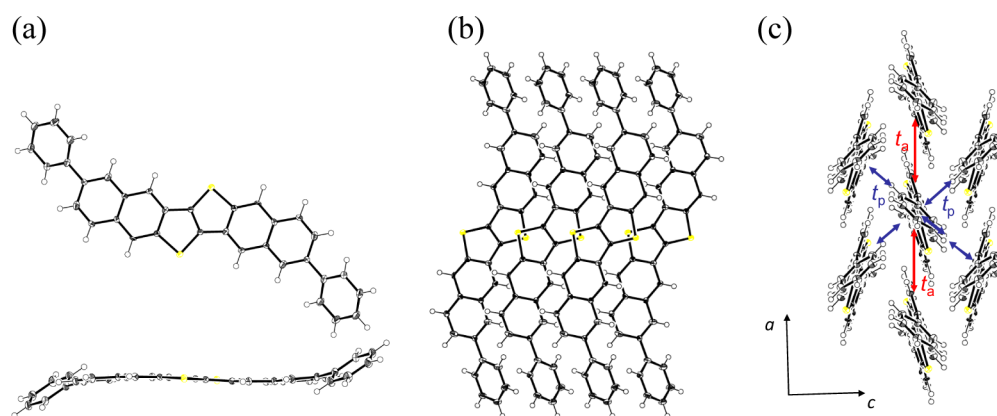


**Figure 3.** (a) Molecular structure, (b) *a*-axis projection of packing structure, and (c) packing structure in the crystallographic *ac*-plane with calculated transfer integrals:  $t_a = 22$  meV and  $t_p = 80$  meV, respectively, of 3,10-DPh-DNTT.

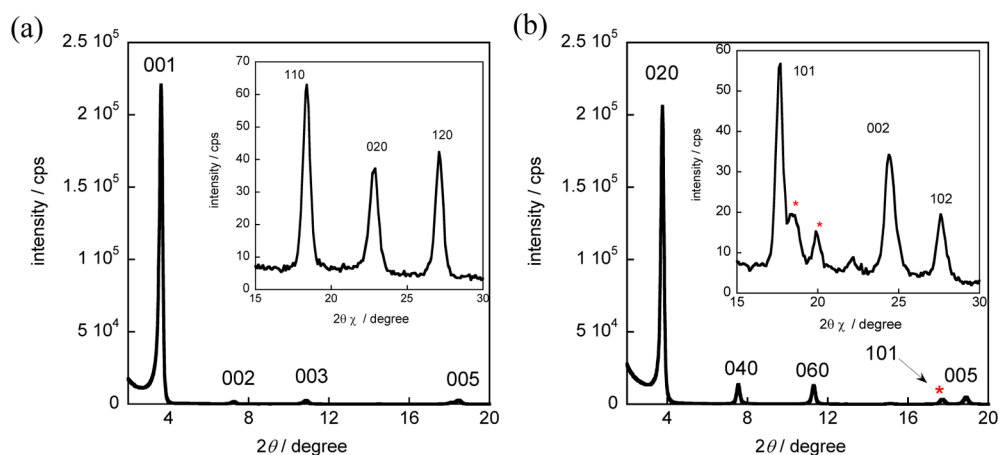


**Figure 4.** Out-of-plane and in-plane (insets) XRD patterns of vapor deposited thin films on Si/SiO<sub>2</sub> substrate surface-modified with octadecyltrichlorosilane for (a) 2,9-DPh-DNTT and (b) 3,10-DPh-DNTT. The asterisked peaks are assigned to miss-oriented crystallites.

to treatment in boiling water, flexible transistors using DNTT as the active material.<sup>6c</sup> However, the transistor characteristics of the DNTT-based transistors were not preserved under thermal treatments above 150 °C. With these results on DNTT-based OFETs, we examined thermal stability of several DNTT derivatives recently developed. As a result, two isomeric diphenyl derivatives of DNTT (DPh-DNTTs, Figure 1)<sup>5c</sup> turned out to be thermally stable organic semiconductor up to 250 °C. We here report characterization of two isomeric DPh-DNTTs, i.e., 2,9- and 3,10-DPh-DNTTs, including their

packing structures, thermal properties, and device characteristics in comparison with the parent and didecyl-DNTTs (C<sub>10</sub>-DNTTs).

## RESULTS AND DISCUSSION

**Packing Structure in Bulk Single Crystals and Thin Films.** Synthetic details and preliminary device characterizations of two isomeric DPh-DNTTs were reported previously.<sup>5c</sup> The packing structures in the bulk crystal and thin film state, however, have not been elucidated yet, and thus

we first carried out their structural characterizations. Single-crystal X-ray analyses of two DPh-DNTTs demonstrated that the compounds have the typical herringbone packing structure with intermolecular interactive short contacts (see Figure S1 in the Supporting Information) in the bulk single-crystal phase as the parent DNTT has (Figures 2 and 3). This contrasts to the isomeric C<sub>10</sub>-DNTTs, where the packing structure is affected by the substitution position. 2,9-C<sub>10</sub>-DNTT crystallizes into a similar herringbone packing structure in the bulk crystals, whereas 3,10-C<sub>10</sub>-DNTT affords a characteristic  $\pi$ -stacking structure, which can be rationalized by its cranklike molecular shape with two decyl groups pointing up and down against the DNTT-core axis.<sup>7</sup> In the present phenyl derivatives, on the other hand, the molecular shapes are less sensitive to the substitution positions, and therefore, the both isomers are roughly linear in molecular shape (Figures 2a and 3a). This can rationalize their preference to take herringbone packing structures in the bulk, being consistent with the fact that DNTT and most of its related materials tend to take a similar herringbone packing.<sup>8</sup>

Vapor deposited thin films on Si/SiO<sub>2</sub> substrates were also investigated by out-of-plane and in-plane X-ray diffractions (XRDs) (Figure 4). Judging from intensive peaks both in the out-of-plane and in-plane XRDs, the thin-films of both isomers are highly crystalline. Most of the major peaks appeared in the thin film XRD patterns are well indexed by the bulk crystallographic cells, and thus it can be concluded that the crystallographic phases in the bulk crystals and thin films on Si/SiO<sub>2</sub> substrates are basically the same. For the 2,9-isomer, all the peaks observed in the out-of-plane XRD are indexed as 00*l* reflections (Figure 4a), and those in the in-plane XRD (Figure 4a inset) are related to the crystallographic *ab* cell, which clearly indicates that the crystallographic *c*-axis stands nearly perpendicular to the substrate surface. This is in fact a common feature of the high performance OTFTs based on related acene and thienoacene organic semiconductors such as pentacene,<sup>9</sup> DNTT, and BTBT derivatives.<sup>8</sup> Similar XRD profiles are also obtained for the 3,10-isomer, but in this case, there are several peaks assignable to mis-oriented crystallites, indicating that structural perfection is better for the 2,9-isomer than the 3,10-isomer.

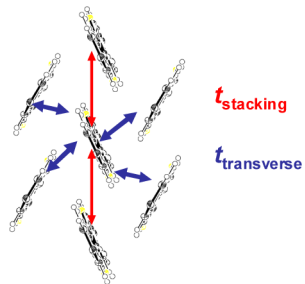
The above XRD studies both in the bulk crystals and vapor deposited thin films clearly indicate that the present materials can be regarded as typical organic semiconductors suitable for thin film transistor application, e.g., edge-on molecular orientation with the molecular long axis being along with the surface normal and two-dimensional herringbone packing in the substrate in-plane direction, which at the same time rationalizes their relatively high mobility of up to 3.5 cm<sup>2</sup> V<sup>-1</sup> s<sup>-1</sup> in our preliminary evaluations.

In order to further understand the electronic structure of these materials, we calculated intermolecular transfer integrals of HOMOs (*t*<sub>HOMO</sub> values) in the herringbone cell, i.e., the crystallographic *ab* cell for the 2,9-isomer and the *ac* cell for the 3,10-isomer, respectively (Figures 2c and 3c), using the fragment method embedded in Amsterdam Differential Functional (ADF) program.<sup>10</sup> The calculation results clearly show that the 2,9-isomer has a quite uniform molecular orbital overlap for every neighboring molecular pair with relatively large *t*<sub>HOMO</sub> values (45 and 52 meV), indicating that the material should have a nicely isotropic two-dimensional electronic structure. On the other hand, for the 3,10-isomer, *t*<sub>HOMO</sub> in the stacking direction designated as *t*<sub>a</sub> (22 meV) is

smaller than those of the transverse direction (80 meV), which indicates that the 3,10-isomer has a less isotropic electronic structure than the 2,9-isomer has, though intermolecular orbital overlap in several directions are quite large. These relatively large intermolecular orbital overlap and mostly isotropic electronic structure in the in-plane direction are consistent with their high mobility in the thin film transistors for both isomers.

To get further insight into the relationship between the intermolecular orbital overlaps and mobility obtained from OTFTs based on DNTT derivatives having a similar herringbone packing structure, mobilities extracted from the thin film transistor characteristics and intermolecular transfer integrals calculated based on the packing structure elucidated by single crystal X-ray analysis are summarized in Table 1.

**Table 1. Maximum Mobility Obtained from the Thin-Film OFETs and Calculated Transfer Integrals of DNTT Derivatives with the Herringbone Packing Structure in the Solid State**



compd	$\mu_{\text{opt}}^a$ (cm <sup>2</sup> V <sup>-1</sup> s <sup>-1</sup> )	<i>t</i> <sub>stacking</sub> (meV)	<i>t</i> <sub>transverse</sub> (meV)
DNTT	~ 3.1 <sup>b</sup>	71	91, 14
2,9-C <sub>10</sub> -DNTT	~ 7.9 <sup>c</sup>	83	51
2,9-DPh-DNTT	~ 3.4	52	45
3,10-DPh-DNTT	~ 3.5	22	80

<sup>a</sup>Mobility recorded for optimized thin-film OFETs. <sup>b</sup>See ref 4b. <sup>c</sup>See ref 5b.

Because of the lower symmetry of the crystallographic unit cell of DNTT, two different *t*<sub>transverses</sub> were calculated, and one of them is relatively small (14 meV). From the present comparisons, it can be concluded that not just large intermolecular transfer integrals, but also the isotropic electronic structure with similar effectiveness of intermolecular orbital overlap in each direction is the key for achieving high mobility in thin film transistors.<sup>11</sup> This can be qualitatively rationalized by considering the fact that the vapor-deposited thin-films, in general, consist of crystallites with random orientations, though the molecular long axis stands perpendicular to the substrate surface; the isotropic intermolecular orbital overlap can compensate such random orientations of crystallites and attain the uniform electronic structures in the thin film. From this viewpoint, two 2,9-disubstituted DNTT derivatives seem to be ideal compounds among the present DNTT-based materials.

#### OFET Devices with Vapor-Deposited Thin Films.

OFET devices with a top-contact, bottom-gate configuration fabricated by vapor-deposition showed typical p-channel transistor characteristics. Table 2 summarizes the transistor characteristics with different device fabrication conditions, e.g., surface treatment of Si/SiO<sub>2</sub> substrate and substrate temperature during deposition (*T*<sub>sub</sub>). Regardless of the

Table 2. FET Characteristics of DPh-DNTTs<sup>a</sup>

material	SAM	$T_{\text{sub}}$ (°C)	$\mu_{\text{FET}}^a$ (cm <sup>2</sup> V <sup>-1</sup> s <sup>-1</sup> )	$I_{\text{on}}/I_{\text{off}}$	$V_{\text{th}}$ (V)
2,9-DPh-DNTT	OTS <sup>b</sup>	rt	0.70–0.80	$5 \times 10^7$	-5.2
		60	0.93–1.13	$2 \times 10^7$	-9.3
		100	1.39–1.44	$3 \times 10^8$	-8.8
		150	2.65–2.85	$2 \times 10^7$	+2.7
		200	2.92–2.98	$2 \times 10^7$	-4.2
2,9-DPh-DNTT	ODTS <sup>b</sup>	rt	0.44–0.50	$3 \times 10^7$	-12
		60	2.95–3.25	$1 \times 10^7$	-11
		100	3.26–3.43	$1 \times 10^9$	-9.4
		150	2.80–2.92	$2 \times 10^7$	-8.0
		200	2.58–2.83	$2 \times 10^7$	-2.8
3,10-DPh-DNTT	OTS <sup>b</sup>	rt	1.23–1.28	$3 \times 10^8$	-17
		60	1.22–1.24	$7 \times 10^8$	-21
		100	1.38–1.60	$3 \times 10^8$	-14
		150	2.05–2.08	$4 \times 10^7$	-7.4
		200	0.85–0.91	$5 \times 10^7$	-10
3,10-DPh-DNTT	ODTS <sup>b</sup>	rt	0.96–1.00	$1 \times 10^8$	-18
		60	0.91–0.96	$5 \times 10^8$	-19
		100	3.42–3.56	$9 \times 10^8$	-17
		150	1.15–1.33	$5 \times 10^7$	-5.7
		200	0.22–0.25	$8 \times 10^6$	-12

<sup>a</sup>Data from more than 8 devices with  $L = 190 \mu\text{m}$  and  $W = 1500 \mu\text{m}$ .

<sup>b</sup>OTS: octyltrichlorosilane, ODTS: octadecyltrichlorosilane.

fabrication conditions, both DPh-DNTTs gave excellent FET characteristics, and the highest mobilities were obtained on the devices fabricated on the octadecyltrichlorosilane (ODTS)-treated substrates at  $T_{\text{sub}} = 100 \text{ }^\circ\text{C}$  for both compounds. These FET characteristics were maintained in air even after 30 days under ambient conditions (Figure 5), indicating their good air stability, which is consistent with their relatively low-lying HOMO energy levels (5.3 eV below the vacuum level) determined by photoelectron yield spectroscopy in air (PESA) with their evaporated thin films (see Figure S2 in the Supporting Information).<sup>12</sup>

**Thermal Stability of OFET Devices Based on DNTT Derivatives.** In the recent advanced application of DNTT-based OFETs, it has been pointed out that thermal stability is

also an important material characteristic for further sophisticated device applications.<sup>6c</sup> We thus tested the thermal stability of DNTT and its derivatives and their OFET devices fabricated on the Si/SiO<sub>2</sub> substrates.

Differential scanning calorimetry (DSC) of the parent DNTT showed no thermal transition over 350 °C,<sup>4a</sup> and so do two DPh-DNTTs, whereas two C<sub>10</sub>-DNTTs showed apparent thermal transition at around 110 °C, which can be assigned to the transition to liquid crystalline (LC) phases (see Figure S3 in the Supporting Information). Because of the thermally induced phase transitions, both C<sub>10</sub>-DNTT-based devices showed significant degradation upon annealing above 100 °C (see Figure S4 in the Supporting Information). In the case of DNTT, although no thermal transition was observed in DSC, the transistor characteristics were degraded significantly on annealing above 150 °C, which is basically consistent with the DNTT-based devices fabricated on flexible substrate previously reported.<sup>6c</sup> The thermal instability of DNTT-based devices is ascribed to subtle changes in the packing structure in the thin film state on substrate confirmed by thin-film XRDs.<sup>6c</sup> In contrast to these transistor characteristics affected by the thermal treatment, the present DPh-DNTT-based OFETs showed excellent stability against the thermal annealing (Figures 6 and 7a). In particular, the 2,9-DPh-DNTT-based OFETs showed no significant degradation in the transfer characteristics and extracted mobilities up to 250 °C, although slight decrease of mobility and negative shift of the threshold voltage ( $V_{\text{th}}$ ) were observed for the 3,10-DPh-DNTT-based OFETs above 200 °C. These excellent thermal stabilities of DPh-DNTTs-based OFETs are of sharp contrast to the C<sub>10</sub>-DNTT-based transistors, which can not preserve the original high performance even on mild thermal treatments ( $\sim 100 \text{ }^\circ\text{C}$ ) (Figure 7a).

These improved thermal stabilities can be understood by the stiffness of the packing structure of DPh-DNTTs in the thin film state. Out-of-plane XRDs of the thin film upon annealing clearly indicate that the molecular orientation in the 2,9-C<sub>10</sub>-DNTT thin film gradually change on annealing, as can be seen from the apparent shifts of the lamella peaks (001 and 002) (Figure 7b). On the other hand, both 2,9- and 3,10-DPh-DNTT thin films show virtually no peak shifts, which is qualitatively consistent with their stable transistor characteristics. The thermally stable packings of the DPh-DNTTs in the

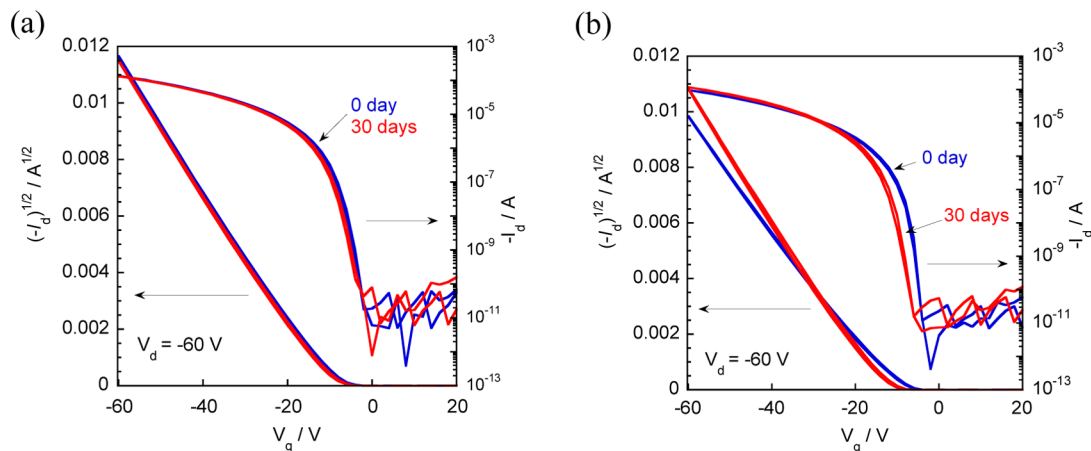


**Figure 5.** Transfer characteristics ( $V_d = -60 \text{ V}$ ) of (a) 2,9- and (b) 3,10-DPh-DNTTs-based OFETs on the ODTS-treated substrate ( $T_{\text{sub}} = \text{rt}$ ): blue traces, freshly fabricated device; red traces, after 30 days storage in ambient conditions.

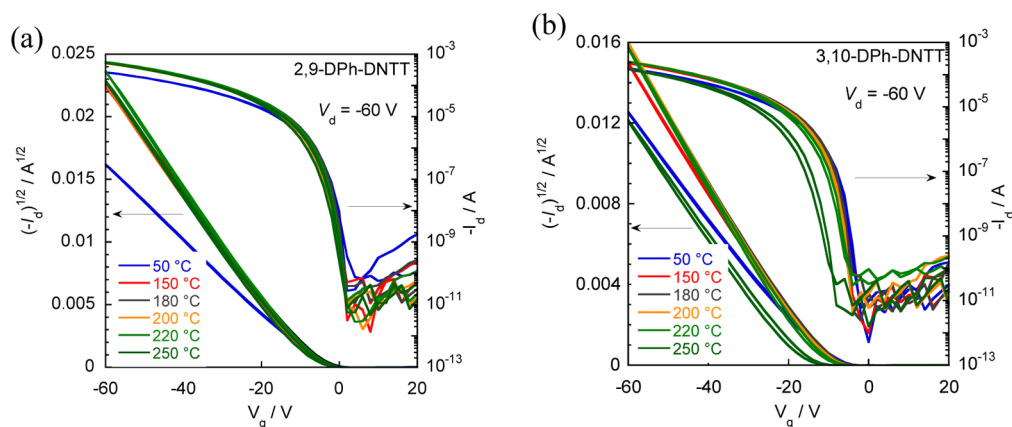


**Figure 6.** Transfer curves of (a) 2,9- and (b) 3,10-DPh-DNTT-based OFETs upon annealing.

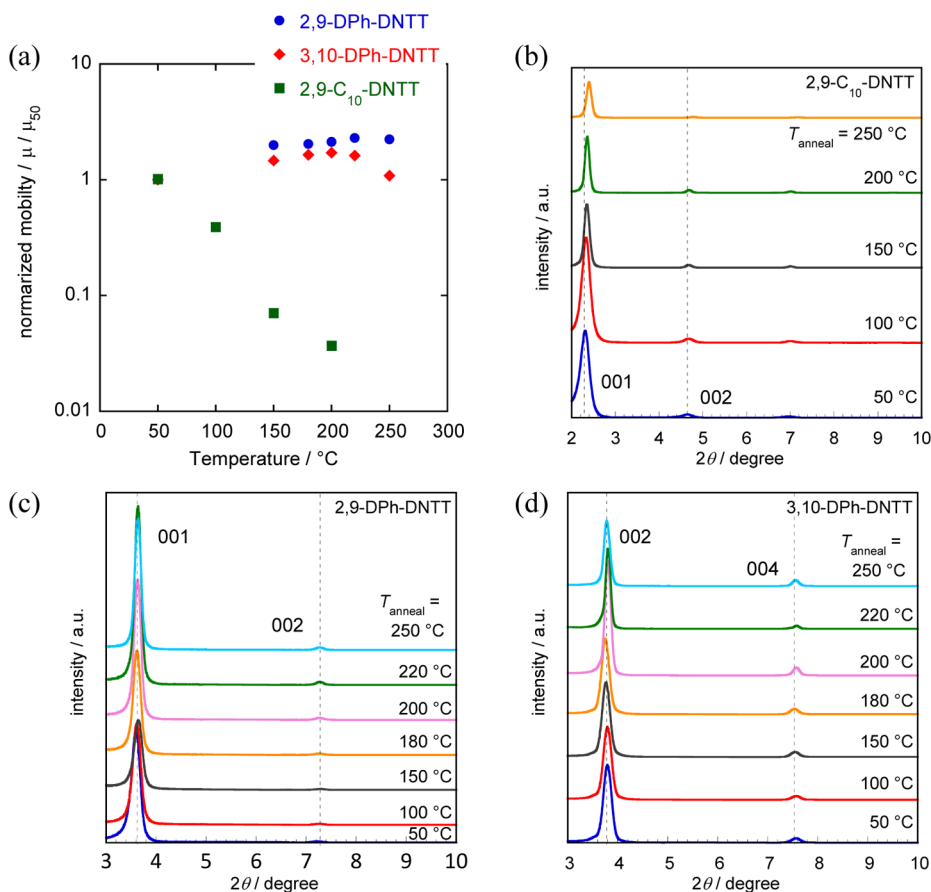


**Figure 7.** Normalized mobility of vapor deposited FET devices using 2,9- $C_{10}$ -DNTT, and two DPh-DNTTs as the active layer on Si/SiO<sub>2</sub> substrate ( $T_{\text{sub}} = \text{rt}$ ) upon annealing at different temperatures for 30 min. (a) Mobilities on annealing at 50 °C were used as the original; out-of-plane XRD patterns upon annealing: (b) 2,9- $C_{10}$ -DNTT, (c) 2,9-DPh-DNTT, and (d) 3,10-DPh-DNTT.

thin film state can be explained by the increase of molecular size with extension of  $\pi$ -conjugation system, which can increase the rigidity of structure in the solid state.

The better thermal stability of the 2,9-isomer above 200 °C than that of the 3,10-isomer can be related to the packing efficiency in the solid state: the 2,9-isomer with more linear-shaped molecular structure can have a dense packing, which reflects the higher density of the 2,9-isomer (1.433 g cm<sup>-3</sup>) than that of the 3,10-isomer (1.397 g cm<sup>-3</sup>), elucidated by the single-crystal X-ray analysis. Also, the molecular structure may affect the packing effectiveness and thermal stability: dihedral

angles between the DNTT core and the phenyl groups are larger for 3,10-isomer (36.4°) than 2,9-isomer (23.4°), and the larger dihedral angle can prevent the dense packing and also induce thermal motion of phenyl groups, both of which may be related to the relatively poor thermal stability of the 3,10-isomer in the high-temperature regime.

## CONCLUSION

In the present work, we have characterized two isomeric DPh-DNTTs by means of the XRD measurements both on single crystals and vapor deposited thin films, and field-effect

transistors, in comparison with the parent and two C<sub>10</sub>-DNTT derivatives. Through these detailed investigations, it turned out that (1) two DPh-DNTTs tend to have the herringbone packing structure both in the bulk single crystal and thin film state regardless the substitution positions; (2) the maximum mobility obtained from the thin-film OFETs of DPh-DNTTs ( $\sim 3.5 \text{ cm}^2 \text{ V}^{-1} \text{ s}^{-1}$ ) is slightly higher than those of the parent DNTT, but lower than those of the decyl derivatives; (3) calculation of intermolecular transfer integrals of HOMO ( $t_{\text{HOMO}}$ s) based on the single-crystal X-ray structures elucidates that DPh-DNTTs afford isotropic two-dimensional electronic structure with relatively large  $t_{\text{HOMO}}$ s in the in-plane direction on the substrate surface, and among two, the 2,9-isomer gives more uniform electronic structure; (4) comparison between the DNTT derivatives possessing a similar herringbone packing affords qualitative correlations between calculated  $t_{\text{HOMO}}$  values and FET mobilities; and (5) thermal stability of the DPh-DNTT-based OFETs was found to be far superior than those of the parent- and C<sub>10</sub>-DNTTs-based ones, and in particular, the 2,9-DPh-DNTT-based OFETs preserves its superior FET characteristics up to 250 °C. For these excellent chemical and thermal stability with superior FET characteristics, we conclude that 2,9-DPh-DNTT is a quite useful organic semiconductor in various applications that require different processes conditions. Further applications of 2,9-DPh-DNTT to various practical devices are now strongly anticipated.

## ■ ASSOCIATED CONTENT

### Supporting Information

Details of device fabrication and crystallographic analyses, crystallographic information files (CIFs) for DPh-DNTTs, ionization potentials (IPs) determined by photoelectron yield spectroscopy in air, DSC traces for DPh-DNTTs, DNTT, and C<sub>10</sub>-DNTTs, FET characteristics of devices based on DNTT and C<sub>10</sub>-DNTTs upon annealing. This material is available free of charge via the Internet at <http://pubs.acs.org>.

## ■ AUTHOR INFORMATION

### Corresponding Author

\*E-mail: [ktakimi@hiroshima-u.ac.jp](mailto:ktakimi@hiroshima-u.ac.jp).

### Notes

The authors declare no competing financial interest.

## ■ ACKNOWLEDGMENTS

This work was financially supported by Grants-in-Aid for Scientific Research (No. 23245041) from MEXT, Japan.

## ■ REFERENCES

- (1) (a) Recent comprehensive reviews on organic semiconductors: (a) Facchetti, A. *Chem. Mater.* **2011**, *23*, 733–758. (b) Wang, C.; Dong, H.; Hu, W.; Liu, Y.; Zhu, D. *Chem. Rev.* **2012**, *112*, 2208–2267.
- (2) (a) Meng, H.; Bao, Z.; Lovinger, A. J.; Wang, B.-C.; Muijsce, A. M. *J. Am. Chem. Soc.* **2001**, *123*, 9214–9215. (b) Takimiya, K.; Kunugi, Y.; Konda, Y.; Ebata, H.; Toyoshima, Y.; Otsubo, T. *J. Am. Chem. Soc.* **2006**, *128*, 3044–3050. (c) Takimiya, K.; Yamamoto, T.; Ebata, H.; Izawa, T. *Sci. Tech. Adv. Mater.* **2007**, *8*, 273–276. (d) Meng, H.; Sun, F.; Goldfinger, M. B.; Jaycox, G. D.; Li, Z.; Marshall, W. J.; Blackman, G. S. *J. Am. Chem. Soc.* **2005**, *127*, 2406–2407.
- (3) (a) Lin, Y. Y.; Gundlach, D. J.; Nelson, S. F.; Jackson, T. N. *IEEE Electron Device Lett.* **1997**, *18*, 606–608. (b) Kelly, T. W.; Boardman, L. D.; Dunbar, T. D.; Muires, D. V.; Pellerite, M. J.; Smith, T. P. *J. Phys. Chem. B* **2003**, *107*, 5877–5881. (c) Payne, M. M.; Parkin, S. R.; Anthony, J. E.; Kuo, C. C.; Jackson, T. N. *J. Am. Chem. Soc.* **2005**, *127*, 4986–4987. (d) Takimiya, K.; Ebata, H.; Sakamoto, K.; Izawa, T.;

- Otsubo, T.; Kunugi, Y. *J. Am. Chem. Soc.* **2006**, *128*, 12604–12605.
- (e) Anthony, J. E. *Angew. Chem., Int. Ed.* **2008**, *47*, 452–483. (f) Gao, P.; Beckmann, D.; Tsao, H. N.; Feng, X.; Enkelmann, V.; Baumgarten, M.; Pisula, W.; Müllen, K. *Adv. Mater.* **2009**, *21*, 213–216. (g) Meng, Q.; Jiang, L.; Wei, Z.; Wang, C.; Zhao, H.; Li, H.; Xu, W.; Hu, W. *J. Mater. Chem.* **2010**, *20*, 10931–10935. (h) Sokolov, A. N.; Atahan-Evrenk, S.; Mondal, R.; Akkerman, H. B.; Sanchez-Carrera, R. S.; Granados-Focil, S.; Schrier, J.; Mannsfeld, S. C. B.; Zombelt, A. P.; Bao, Z.; Aspuru-Guzik, A. *Nat. Commun.* **2011**, *2*, 437.
- (4) (a) Yamamoto, T.; Takimiya, K. *J. Am. Chem. Soc.* **2007**, *129*, 2224–2225. (b) Yamamoto, T.; Takimiya, K. *J. Photopolymer Sci. Tech.* **2007**, *20*, 57–59. (c) Yamamoto, T.; Shinamura, S.; Miyazaki, E.; Takimiya, K. *Bull. Chem. Soc. Jpn.* **2010**, *83*, 120–130.
- (5) (a) Kang, M. J.; Yamamoto, T.; Shinamura, S.; Miyazaki, E.; Takimiya, K. *Chem. Sci.* **2010**, *1*, 179–183. (b) Kang, M. J.; Doi, I.; Mori, H.; Miyazaki, E.; Takimiya, K.; Ikeda, M.; Kuwabara, H. *Adv. Mater.* **2011**, *23*, 1222–1225. (c) Niimi, K.; Kang, M. J.; Miyazaki, E.; Osaka, I.; Takimiya, K. *Org. Lett.* **2011**, *13*, 3430–3433.
- (6) (a) Zschieschang, U.; Ante, F.; Yamamoto, T.; Takimiya, K.; Kuwabara, H.; Ikeda, M.; Sekitani, T.; Someya, T.; Kern, K.; Klauk, H. *Adv. Mater.* **2010**, *22*, 982–985. (b) Zschieschang, U.; Yamamoto, T.; Takimiya, K.; Kuwabara, H.; Ikeda, M.; Sekitani, T.; Someya, T.; Klauk, H. *Adv. Mater.* **2011**, *23*, 654–658. (c) McCarthy, M. A.; Liu, B.; Rinzler, A. G. *Nano Lett.* **2010**, *10*, 3467–3472. (d) McCarthy, M. A.; Liu, B.; Donoghue, E. P.; Kravchenko, I.; Kim, D. Y.; So, F.; Rinzler, A. G. *Science* **2011**, *332*, 570–573. (e) Kuribara, K.; Wang, H.; Uchiyama, N.; Fukuda, K.; Yokota, T.; Zschieschang, U.; Jaye, C.; Fischer, D.; Klauk, H.; Yamamoto, T.; Takimiya, K.; Ikeda, M.; Kuwabara, H.; Sekitani, T.; Loo, Y.-L.; Someya, T. *Nat. Commun.* **2012**, *3*, 723–1–7.
- (7) Kang, M. J.; Miyazaki, E.; Osaka, I.; Takimiya, K. *Jpn. J. Appl. Phys.* **2012**, *51*, 11PD04.
- (8) (a) Ebata, H.; Izawa, T.; Miyazaki, E.; Takimiya, K.; Ikeda, M.; Kuwabara, H.; Yui, T. *J. Am. Chem. Soc.* **2007**, *129*, 15732–15733. (b) Izawa, T.; Miyazaki, E.; Takimiya, K. *Adv. Mater.* **2008**, *20*, 3388–3392. (c) Shinamura, S.; Osaka, I.; Miyazaki, E.; Nakao, A.; Yamagishi, M.; Takeya, J.; Takimiya, K. *J. Am. Chem. Soc.* **2011**, *133*, 5024–5035. (d) Niimi, K.; Shinamura, S.; Osaka, I.; Miyazaki, E.; Takimiya, K. *J. Am. Chem. Soc.* **2011**, *133*, 8732–8739.
- (9) (a) Yoshida, H.; Sato, N. *Appl. Phys. Lett.* **2006**, *89*, 101919–3. (b) Yoshida, H.; Inaba, K.; Sato, N. *Appl. Phys. Lett.* **2007**, *90*, 181930–3.
- (10) (a) ADF2008.01, SCM, *Theoretical Chemistry*, Vrije Universiteit, Amsterdam, The Netherlands, <http://www.scm.com>. (b) Senthilkumar, K.; Grozema, F. C.; Bickelhaupt, F. M.; Siebbeles, L. D. A. *J. Chem. Phys.* **2003**, *119*, 9809–9817. (c) Prins, P.; Senthilkumar, K.; Grozema, F. C.; Jonkheijm, P.; Schenning, A. P. H. J.; Meijer, E. W.; Siebbeles, L. D. A. *J. Chem. Phys. B* **2005**, *109*, 18267–18274.
- (11) Takimiya, K.; Shinamura, S.; Osaka, I.; Miyazaki, E. *Adv. Mater.* **2011**, *23*, 4347–4370.
- (12) Usta, H.; Risko, C.; Wang, Z.; Huang, H.; Deliomeroglu, M. K.; Zhukhovitskiy, A.; Facchetti, A.; Marks, T. J. *J. Am. Chem. Soc.* **2009**, *131*, 5586–5608.